Electronic Supplementary Information (ESI)

Contents

1. Experimental Section

1.1. Reagents and materials

All reagents and materials are of analytical grade and used as received from commercial sources without further purification. H_4EBTC was synthesized according to the method published before.[1]

1.2. Physical measurements

Thermal gravimetric analyses (TGA) were performed using a DTA–TGA 2960 thermogravimetric analyzer in nitrogen atmosphere with a heating rate of 10 °C/min from 30 to 700 °C. Powder X–ray diffraction (PXRD) data were recorded on a Bruker D8 Discover diffractometer with Cu Kα (λ = 1.54056 Å) radiation with a scan speed of 5 °/min and a step size of 0.02° in 2θ. Elemental analyses (C, H) were carried out on a Perkin–Elmer 240 analyzer. The IR spectra were obtained on a NICOLET iS10 spectrometer in the 4000–400 cm^{-1} region. UV/visible absorbance was collected in the solid state at room temperature on a Perkin–Elmer Lambda 950 UV/vis spectrometer equipped with Labsphere integrating over the spectral range 200–800 nm using KBr pellet as reflectance standards. Steady state emission and excitation spectra were recorded for the solid samples on an F–7000 FL spectrophotometer equipped with a 150 W Xenon lamp as an excitation source at room temperature. The photomultiplier tube (PMT) voltage was 700 V in all the measurements. The scan speed was 1200 nm/min. The phosphorescence lifetime measurement and absolute photoluminescence quantum yields were measured on Steady–State & Time–Resolved Fluorescence Spectrofluorometer.

2. Preparation and characterization of 1

[Mn_3(HEBTC)$_2$(DMSO)$_6$] (1). A solution of $MnCl_2 \cdot 4H_2O$ (4.2 mg, 0.028 mmol), H_4EBTC (5 mg, 0.014 mmol), DMSO (0.4 mL), CH_3OH (0.10 mL), HNO_3 (0.02 mL, 1M in DMF) and H_2O (0.10 mL) were mixed and sealed in a 10 mL Teflon–lined autoclave and heated to 110 °C for 24 h. The light yellow rectangle–shaped crystals were achieved after slowly cooled to room temperature (yield: 75 % based on Mn).

Anal. Calcd for $C_{48}H_{50}Mn_3O_{22}S_6$: C, 43.15; H, 3.77. Found: C, 43.10; H, 3.90. Selected IR data (KBr pellet, cm^{-1}): 3444 (b), 3074 (w), 3002 (w), 2915 (w), 1706 (s), 1616 (w), 1577 (w), 1355 (w), 1004 (s), 982 (w), 775 (s), 723 (s).

3. Crystal Structure Determination

Suitable single crystal of **1** was carefully selected under an optical microscope and glued to thin glass fibers. Single crystal X–ray diffraction data were collected on a Bruker Smart Apex II CCD diffractometer at 293 K using graphite monochromated Mo/Kα radiation (λ = 0.71073 Å). Data reductions and absorption corrections were performed with the SAINT[2] and SADABS2[3] software packages, respectively. Structures were solved by a direct method using the SHELXL–97 software package.[4] The non–hydrogen atoms were anisotropically refined using the full–matrix least–squares method on F^2. All hydrogen atoms were placed at the calculated positions and refined riding on the parent atoms.
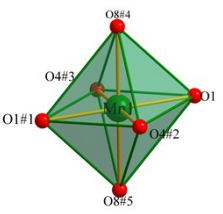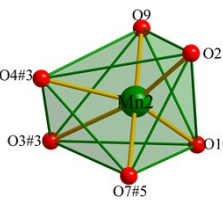
CCDC–1584148 (**1**) contains the supplementary crystallographic data for this paper. These data can be obtained free of charge via www.ccdc.cam.ac.uk/data_request/cif. The crystallographic data and details of structural refinement for **1** are listed in Table S1 and selected bond distances and angles are summarized in Table S2.

Table S1: Crystallographic data and structural refinements for **1**

Formula	$C_{48}H_{50}Mn_3O_{22}S_6$
Formula weight	1336.06
CCDC no.	1584148
Temperature (K)	296(2)
Wavelength (Å)	0.71073
Crystal size /mm	0.21×0.20×0.19
Crystal system	Triclinic
Space group	*P−1*
a / Å	9.728(3)
b / Å	12.452(3)
c / Å	12.917(3)
α / (°)	90.806(4)
β / (°)	107.260(3)
γ / (°)	110.609(3)
V / Å³	1386.3(6)
Z	1
F(000)	685
$\theta_{min,max}$/°	1.67 −25.01
GOF	1.041
$R_1{}^a$, w$R_2{}^b$ [$I > 2\sigma(I)$]	0.0808, 0.2060

$^aR_1 = \sum||F_0| - |F_c||/\sum|F_0|$; $^bwR_2 = \{\sum[w(F_0{}^2 - F_c{}^2)^2]/\sum[w(F_0{}^2)^2]\}^{1/2}$

Table S2: Selected bond lengths (Å) and angles (º) in **1**

|	Bond lengths (Å)		Bond angles (º)			
	Mn1–O1	2.120(4)	O1–Mn1–O4#3	83.9(15)	O1–Mn1–O4#3	83.9(15)
		2.153		84.205		84.205
	Mn1–O1#1	2.120(4)	O1–Mn1–O8#4	86.8(17)	O1#1–Mn1–O8#4	86.8(17)
		2.153		84.767		84.767
	Mn1–O8#4	2.178(4)	O8#4–Mn1–O4#2	89.1(14)	O8#4–Mn1–O4#3	90.9(14)
		2.209		93.461		86.539
	Mn1–O8#5	2.178(4)	O1–Mn1–O4#2	96.1(15)	O1–Mn1–O4#2	96.1(15)
		2.209		95.795		95.795
	Mn1–O4#2	2.193(4)	O1–Mn1–O8#5	93.2(17)	O1#1–Mn1–O8#5	93.2(17)
		2.219		95.233		95.233
	Mn1–O4#3	2.193(4)	O1–Mn1–O1#1	180.0(1)	O8#4–Mn1–O8#5	180.0(1)
		2.219		180		180
	Bond lengths (Å)		Bond angles (º)			
	Mn2–O2	2.156(4)	O10–Mn2–O9	85.8(2)	O9–Mn2–O4#3	87.6(18)
		2.172		82.036		84.687
	Mn2–O9	2.152(5)	O9–Mn2–O2	89.2(18)	O7#5–Mn2–O10	92.2(2)
		2.302		87.854		93.598
	Mn2–O10	2.112(5)	O7#5–Mn2–O2	93.5(17)	O7#5–Mn2–O4#3	92.8(16)
		2.148		93.957		98.719
	Mn2–O7#5	2.103(5)	O10–Mn2–O2	103.3(2)	O2–Mn2–O4#3	111.7(15)
		2.130		104.465		104.953
	Mn2–O3#3	2.535(4)	O10–Mn2–O4#3	144.3(1)	O7#5–Mn2–O9	177.0(17)
		2.522		147.111		175.576
	Mn2–O4#3	2.204(4)				
		2.231				

Notes: black color data obtained from single crystal X–ray diffraction and blue color data got from geometry optimaization. Symmetry transformations used to generate equivalent atoms for **1**: #1=–x, –y, 1–z; #2=1–x, –y, 1–z; #3=–1+x, y, –z; #4=1–x, –y, 2–z; #5=–1+x, y, –1+z.
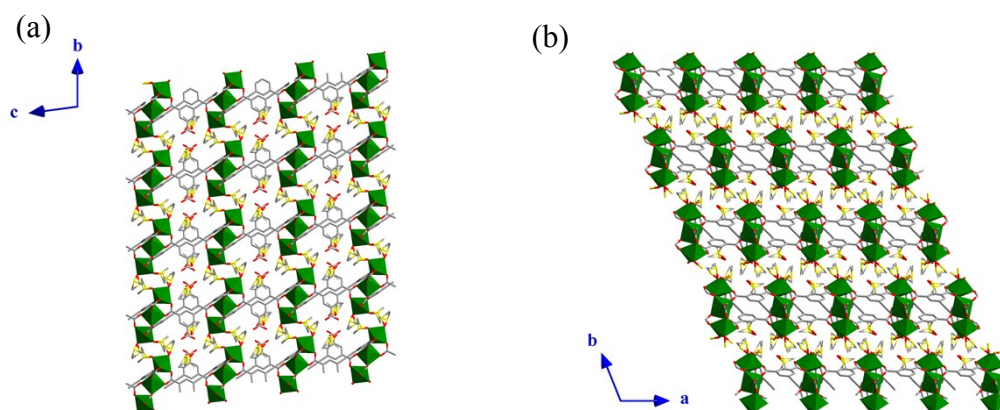
4. Crystal structure
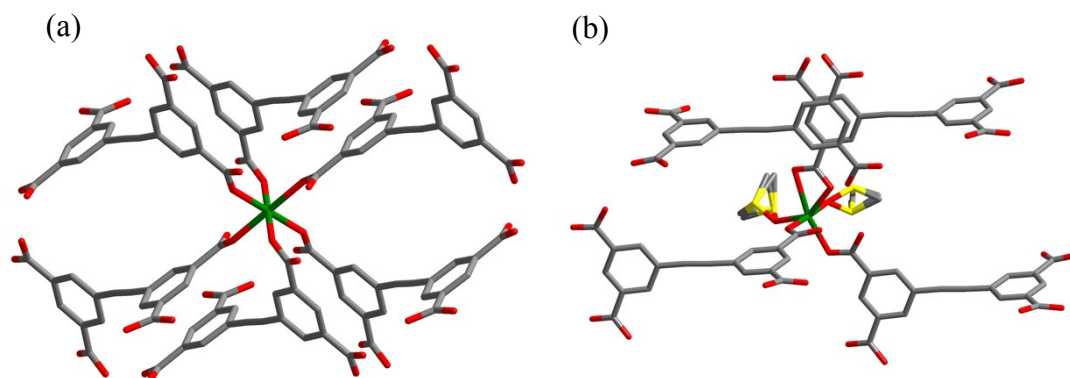
Fig. S1 Coordination environments of (a) Mn1 and (b) Mn2 ions in **1**.
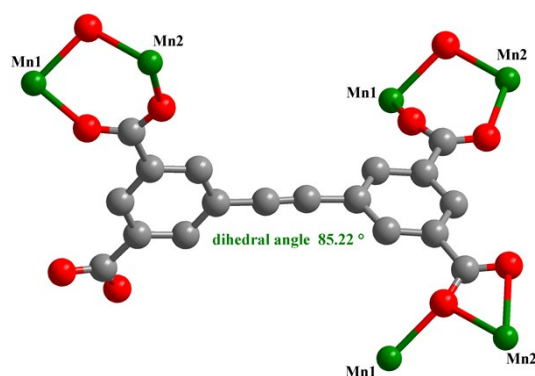
Fig. S2 Binding modes of the ligand in **1** and the dihedral angle between two phenyl rings in HEBTC^{3-} ligand (all hydrogen atoms are omitted for clarity).


Fig. S3 Crystal packing structure of **1** viewed along (a) *a–axis* and (b) *c–axis* (all H atoms are omitted for clarity).

5. Characterizations

5.1 PXRD Patterns

The powder X–ray diffraction (PXRD) experiments for CP **1** was carried out carefully to check phase purity at room temperature. The patterns showed that the main peaks of the synthesized CP was closely consistent with that of the simulation from the single–crystal X–ray diffraction data, which imply high quality of the obtained products (Fig. S4). The difference in reflection intensities is probably due to the preferred orientation effects.
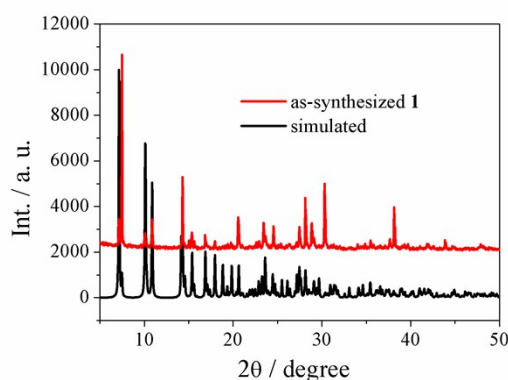
Fig. S4 PXRD patterns of simulated from X−ray single−crystal structure data and as–synthesized sample of **1** at ambient temperature.

5.2 IR Spectrum
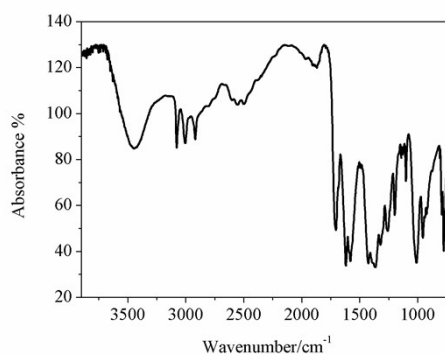
Fig. S5 IR spectrum of **1** recorded using KBr pellet.

5.3 Thermogravimetric analysis

The thermal stability of **1** was also detected *via* thermogravimetric analysis (TGA). The thermal analysis of powdered sample of **1** was performed under a nitrogen atmosphere. From the TG curve depicted in Fig. S6, the thermogravimetric analysis of **1** indicates a weight loss of 11.63 % in the temperature range 25–212 °C (calcd. 11.70 %) for **1**, which corresponds to the loss of uncoordinated DMSO molecules. The gradually losing weight still undergoes upon further heating, and this process may be related to a continuous release of coordinated DMSO molecules with a weight loss of 23.45 % between 212 and 418 °C (calculated 23.39 %). Therefore, the TG profiles of **1** do not show a clear step corresponding to the loss of included solvents. After the departure of the coordinated DMSO molecules, the frameworks begin to collapse.
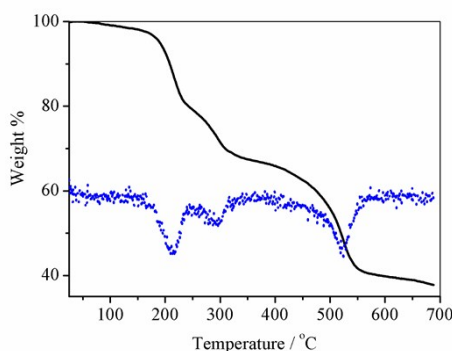

Fig. S6 TG and DTA (dash line) plots of **1** in the ranges of 25-700°C.

5.4 Photophysical properties

Fig. S7 depicts the electronic absorption spectra of H_4EBTC and CP **1** in solid state. As was already reported in the literature, H_4EBTC exhibits broad absorption in the ranges of 200–400 nm and one characteristic, prominent band located at 280 nm, which may be assigned to the intraligand $\pi \rightarrow \pi^*$ transitions of the aromatic rings. In the case of **1**, these bands are not strongly perturbed upon its coordination to MnII, however, a little blue–shift of is observed.
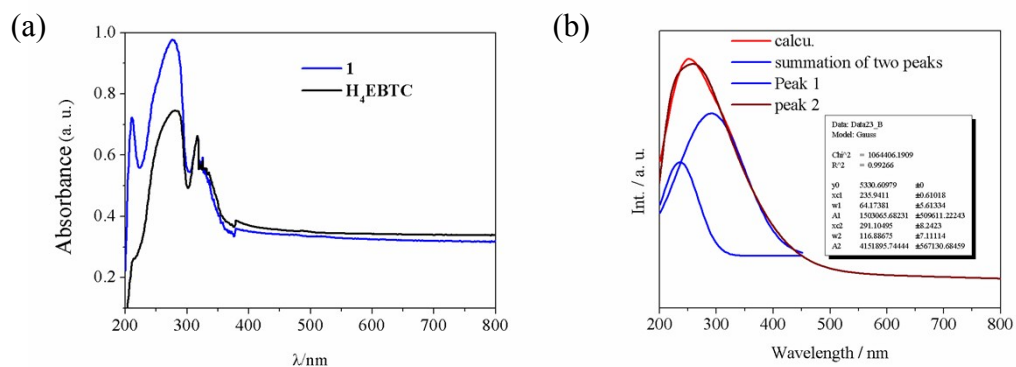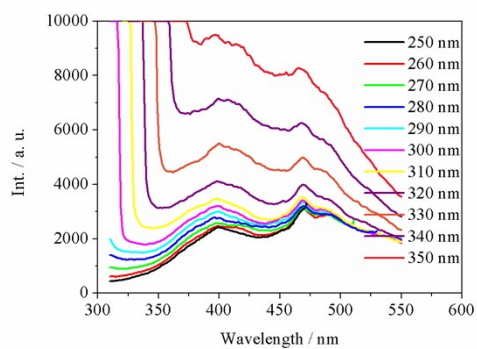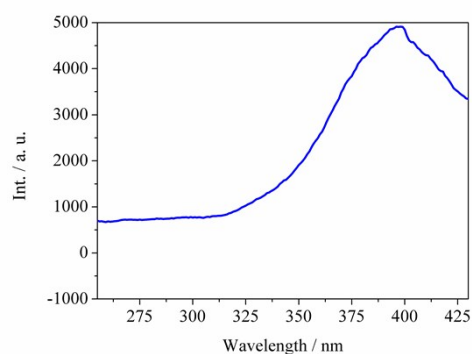
Fig. S7 (a) UV−vis absorption spectra for **1** (blue) and the H$_4$EBTC ligand (black) and (b) the calculated absorption spectrum of **1**.
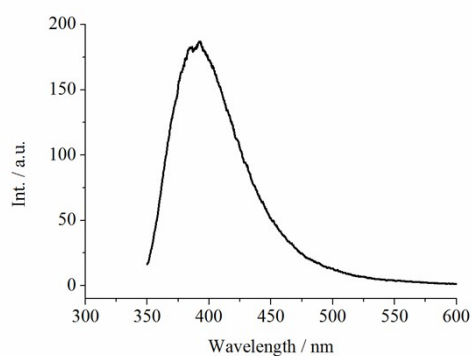
Fig. S8 The solid−state PL spectra of H$_4$EBTC (λ_{ex}= 278 nm) at room temperature.

Fig. S9 Solid−state PL spectra of **1** by variation of excitation light under the same determining conditions.

Fig. S10 Solid–state excitation spectra of **1** at room temperature, monitored at 470 nm.

Table S3: Summary of luminescent MOFs/CPs

MOFs/CPs	λ_{ex} (nm)	λ_{em} (nm)	Quantum yield (%)	Ref.
$[Mn_3(bipo^-)_4(SCN)_2]_n$	365	458	7.8	5
$Mn(bpy)(H_2L)_2(H_2O)_2$	350	460	6.16	6
Mn–L	320	410	8.3	7

Details of crystal structure optimization and band structure calculation

The geometry optimization of crystal structure and the calculation of electron band structure were performed for **1** in the DFT framework. The electron band structure and the density of states were calculated for **1** based on the optimized crystal structure. The total plane–wave pseudopotential method forms the basis of the CASTEP calculations. The exchange–correlation effects were treated within the generalized gradient approximation (GGA) with the Perdew–Burke–Ernzerhof (PBE) functional.[8] The long–range van der Waals (vdW) interactions corrections were utilized the Grimme's semi–empirical approach (DFT–D).[9] The plane–wave basis set energy cutoff were set at 300 eV for **1**. The convergence parameters were set as follows: the SCF tolerance 1×10^{-6} eV/atom, the total energy tolerance 2×10^{-5} eV/atom, the maximum force tolerance 0.05 eV/Å, the maximum stress component 0.1 GPa and the displacement of convergence tolerance 0.002 Å. Other calculation parameters were set at the default values in the CASTEP code.

In the process of geometric optimization, the unit cell parameters of **1** were constrained to the values obtained from the X–ray single crystal diffraction at 296 K,

the positions of all atoms were fully optimized. The initial positions of all atoms were directly taken from the single crystal structure data of **1** at 296 K for geometry optimization. The DMSO molecules in lattice were removed in the calculated structure. The coordination DMSO molecules show highly disordered with two possible positions in the single crystal structure at 296 K, however, one of two parts was removed for each DMSO molecules in the geometry optimization process. The optimized bond lengths and the bond angles are listed in Table S2, which are comparable to the results obtained from the single crystal analysis at 296 K.

6. References

1. Y. X. Hu, S. C. Xiang, W. W. Zhang, Z. X. Zhang, L. Wang, J. F. Bai and B. L. Chen, *Chem. Commun.,* 2009, **48**, 7551.
2. Bruker, APEX 2, SAINT, XPREP, Bruker AXS Inc., Madison, Wisconsin, USA, 2007.
3. Bruker, SADABS, Bruker AXS Inc., Madison, Wisconsin, USA, 2001.
4. G. M. Sheldrick, SHELXS97 and SHELXL97: Program for the refinement of crystal structure, University of Göttingen, Germany, 1997.
5. G. P. Yong, Y. Z. Li, W. L. She, and Y. M. Zhang. *Chem. Eur. J.* 2011, **17**, 12495.
6. F. F. Zhao, H. Dong, B. B. Liu, G. J. Zhang, H. Huang, H. L. Hu, Y. Liu and Z. H. Kang, *CrystEngComm,* 2014, **16**, 4422.
7. A. Bajpai, A. Mukhopadhyay, M. S. Krishna, S. Govardhan and J. N. Moorthy, IUCrJ 2015, **2**, 552.
8. J. P. Perdew, K. Burke and M. Ernzerhof, *Phys. Rev. Lett.,* 1996, **77**, 3865.
9. S. J. Grimme, *Comput. Chem.,* 2006, **27**, 1787.